Research Project [3]

Connectivity effects for NFkB-NrF2 crosstalk, a quantitative Petri-Net analysis approach

Carlos Andres Mariscal Melgar

Student I.D. 200692669

Supervisor: [Dr Steven Webb]

Internal Assessor: [Dr. Chris Goldring]

Strand: [Drug Safety]

Word Count: [3800]

Connectivity effects for NFkB-NrF2 crosstalk, a quantitative Petri-Net analysis approach.

Abstract:

Nuclear factor kappa B (NFkB) is a critical regulator of the cellular response against cellular stress and infection and Nuclear factor erythroid 2–related factor 2(Nrf2) is a master regulator of transcriptional activation of genes encoding cytoprotective proteins. A Petri-Net model was created to include the Nrf2-NFkB crosstalk modules. Simulated using the Gillespie Algorithm to provide a stochastic simulation of Token flow in the flattened Petri-Net finalizing in observation of asynchronous behaviour in Nrf2-NFkB crosstalk is observable in assumptions which included *de* novo Nrf2 synthesis inhibition by NFkB and, GSK3B induction by NFkB, comparison with a Ordinary Differential equations (ODE) model of NFkB oscillatory behaviour was also performed.

Introduction

The purpose of this project is to build an *in silico* non-parameterised model of the cross-talk between the regulatory pathways ,Nuclear Factor Kappa B (NFkB) and Nuclear factor erythroid 2–related factor 2(Nrf2), and whether asynchronous Oscillations can occur between them, Ultimately providing experimentalists with insight into oscillatory behaviour of these pathways, and if it does indeed occur which elements would be worth pursuing further.

NFkB is the generic name used for a family of evolutionarily conserved transcription factors that function through dimerization and ultimately regulate genes that are involved in immunity, inflammation, cell survival, proliferation, differentiation and, apoptosis (3, 4). Because chronic inflammatory diseases and cancer often have NFkB involvement and, since NFkB is a key regulator in oncogenesis by promoting proliferation and inhibiting apoptosis (5), NFkB and its associated proteins have become desirable targets for the development of novel drugs and therapeutics (5-7). NFkB belongs to the Rel family of proteins which encompasses 5 different mammalian proteins namely: p65, C-Rel, RelB, NFkB1 (p50/p105) and NFkB2 (p52/100) (3). Synthesis of these proteins occurs with p105 and p100 being synthesised as large precursors to p50 and p52 with p65, C-

Rel and, RelB being synthesised in a mature form.

The NFkB pathway like the Nrf2 pathway can be targeted upstream or downstream with the ultimate aim of changing the flux of information to obtain the desired response, thus allowing all associated pathways to be potential drug targets (6). NFkB can be activated by numerous pathways, the most commonly associated factor that induces NFkB activity are the tumour necrosis factor-alpha (TNF-α) (8). Although the tumour necrosis factor superfamily is all able to induce the NFkB pathway (8) and can also be activated by interleukin-1 (IL-1) (9) as well by-products of bacterial and viral infections (3).In this particular instance,
NFkB activation involves a signal dependant activation of the IkappaB kinase (IKK)(4, 8). The IKK complex is composed of three subunits IKKα, KKβ and, IKKγ (3). IKKα and IKKβ are the catalytic subunits of the IKK complex whereas IKKγ is the regulatory subunit. Catalytic activity by IKKβ is essential for the activation of the pathway, which occurs on serine residues 19 and 21 of the N-terminal in IkBb and serine residues 32 and 36 for IkBa) (3, 8) IKK activation is therefore essential for NFkB activation, since activation of IKK can occur through the same stimuli that activates NFkB, such as inflammatory cytokines, and by-products of microbial, fungal and viral infections (3). Once NFkB is activated through phosphorylation of the IkB inhibitory protein, IkBa is ubiquitinated and primed for destruction by the proteasome (8, 10) and, activated NFkB is translocated into the nucleus where it can regulate transcription (10) and, leading to a physiological response such as a immune response (3).

Methods

Systems Biology is an emergent field in the biosciences. Coined earlier in the 20th century, the meaning now encompasses a broad interdisciplinary field where engineering, mathematics and, computer science collide with experimental biology.
Quantitative petri-nets were the chosen method for this study.
In order to study the Petri-Nets *Snoopy* a quantitative Petri-net analysis software was used(11).

A Petri-Net is a weighted, directed bipartite graph and, it consists of the following elements (Figure 1).

There are two types of *Nodes*, which are *Places* or *Transitions*, graphically represented by a circle and a square respectively. places are used to represent passive elements of the system, be it substrates, catalysts, precursors or products of the chemical reactions(11) whilst transitions are used to represent dynamic components of the system, such as chemical reactions, transport of compounds through organelles and phase transitions or other transformations. To model a reversible reaction two opposite transitions would be used.

Each place contains an arbitrary amount of *Tokens*, represented as black dots, or a natural number. Unless specified the token value is set to zero by default. The amount of tokens in a *place* can be used to represent the concentration or number of molecules present of that particular compound.

Edges or *Arcs* are used to connect the Petri-Net, they can connect nodes of different types, they go from precursor (Pre-places) to reactions (transitions) and from reactions (transitions) to

products (Post-places). The arcs on a petri-net are weighted by natural numbers, the arc weight represents known stoichiometry of reactions taking place, or other semi-quantitative assumptions, an arc weigh of 1 is set as default on a Petri-Net.

On an extended Petri-Net different types of arcs can be used to represent different behaviour.
Read Arc, which is represented by a black dot instead of an arc head, acts by imposing a condition on the transition it interacts with, e.g., the conformation of a protein complex determines whether a reaction can occur, or the reaction is conditional upon an enzyme (Figure 2), places connected to transitions through a read arc allow that transition to fire only if the minimum threshold is met (given by the arc's weight) and does not change the number of tokens present in the read-connected place.

Inhibitor Arc, represented by a hollow dot instead of an arch head, acts similar to a read arc, with the fundamental difference that it does not allow the transition to fire if the inhibitor arc connected pre-place is over the threshold (given by the inhibitor arch weight) and thus represents all types of biological inhibition.

A modifier arc can be used only when studying stochastic petri-nets, it does not allow weights to be adjusted, however it adjusts the fire-rate based on the amount of tokens present in the Pre-place connected to it, thus representing stochastic behaviour more accurately.

Finally Scheduled Transitions were used in this model, their properties allow a time/fire count associated delay to be pre-set on these transitions thus allowing other events to occur without firing, this allows the system to reach a steady state which then is perturbed by the firing of the scheduled transition.

As it is shown in Figure 2, Petri-Net graphical notation can be used to accurately describe molecular events such as transcription and translation, thus being appropriate for the study of signalling pathways (12).

The Nrf2 model (Figure 3) was done as described in table 1. The NFkB model (Figure 3) was done as described in table 2.

Table 1: Nrf2 Petri-Net model, where I= inhibitor arc, R= read arc, A=arc, T=transition, S=Scheduled transition, (initial token set at 10 in place Nrf2).

Pre-Place->(arc type)	Transition type and Schedule	Pre-Place Arc type & weigh ; Post-Place Arc type & weigh	Post-Place
(none)	T->0	None ; A=10	Nrf2
Nrf2->(A)	S->20,1,30	A=1 ; A=1	Nrf2p
Nrf2->(A),GSK3B->I	T->0	A=1,I=1 ; A=1	Nrf2p
(none)	T->0	None ; A=1	GSK3B
GSK3B->(A)	T->0	A=1 ; A=1	Sink
GSK3B->(A)	S->20,1,30	A=1 ; A=1	GSK3Bp
GSK3Bp->(A)	T->0	A=1 ; None	(none)
Nrf2p->(A)	T->0	A=1 ; A=1;	nNrf2p
Nrf2->(A)	T->0	A=1 ; A=1	nNrf2

nNrf2->(A)	T->0	A=1 ; A=1	nNrf2p
nNrf2p->(A)	T->0	A=1 ; A=1	nNrf2pp
nNrf2pp->(A)	T->0	A=1 ; None	(none)
(none)	T->0	None ; A=1	Keap1
Keap1->(A)	S->0,1,10	A=1 ; None	(none)
Keap->(A),Nrf2->(A)	T->0	A=1,A=1 ; A=1	Nrf2Keap1
Nrf2Keap1->(A)	T->0	A=1 ; A=1	Keap1
Keap1->(A)	T->0	A=1 ; A=1	Sink

Table 2: NFkB Petri-Net model, where I= inhibitor arc, R= read arc, A=arc, T=transition, S=Scheduled transition, (initial token set at 100 in place IKKn and, 100 in place IkBaNFkB).

Pre-Place->(arc type)	Transition type and Schedule	Pre-Place Arc type & weigh ; Post-Place Arc type & weigh	Post-Place
IKKn->(A)	S->20,1,30	A=10 ; A=10	IKKa
IKKa->(A)	T->0	A=1 ; A=1	IKKi
IKKi->(A),A20->(I)	T->0	A=1,I->1 ; A=1	IKKn
tIkBa->(R)	T->0	R=1 ; A=1	IkBa
IkBa->(A)	T->0	A=1 ; A=1	Sink
IkBa->(A),IKKa->(R)	T->0	A=1 ; A=1	pIkBa
pIkBa->(A)	T->0	A=1 ; None	(none)
IKKa->(R),IkBaNFkB->(A)	T->0	R=1,A=1 ; A=1	pIkBaNFkB
pIkBaNFkB->(A)	T->0	A=1 ; A=1	NFkB
IkBaNFkB->(A)	T->0	A=1 ; A=1	NFkB
IkBaNFkB->(A)	T->0	A=1 ; A=1,A=1	NFkB, IkBa
NFkB->(A),IkBa->(A)	T->0	A=1,A=1 ; A=1	IkBaNFkB
nIkBaNFkB->(A)	T->0	A=1 ; A=1	IkBaNFkB
NFkB->(A)	T->0	A=1 ; A=1	nNFkB
nNFkB->(A)	T->0	A=1 ; A=1	NFkB
IkBa->(A)	T->0	A=1 ; A=1	nIkBa
nIkBa->(A)	T->0	A=1 ; A=1	IkBa
nIkBa->(A)	T->0	A=1 ; A=1	Sink
nIkBa->(A),nNFkB->(A)	T->0	A=1,A=1 ; A=1	nIkBanNFKB
nIkBanNFkB->(A)	T->0	A=1 ; A=1,A=1	nIkBa, nNFkB
nIkBanNFkB->(A)	T->0	A=1 ; A=1	nNFkB
nNFkB->(R)	T->0	R=1 ; A=1	tA20
(none)	T->0	None ; A=1	tA20
tA20->(A)	T->0	A=1 ; A=1	Sink
tA20->(R)	T->0	R=1 ; A=1	A20
A20->(A)	T->0	A=1 ; A=1	Sink
nNFkB->(R)	T->0	R=1 ; A=1	tIkBa
(none)	T->0	None ; A=1	tIkBa
tIkBa->(A)	T->0	A=1 ; A=1	Sink

In order to further validate the Petri-Net Model an alternative model was explored, from rotation 1. This model was done in Matlab which is one of the most widely used numerical platforms in science and engineering,

Matlab's scripting language was used to code an Ordinary Differential

Equations (ODE) model for the NFkB pathway(Figure 6, parameterisation and reactions detailed in annex), in order to help validate the non-parameterised Petri-net model output.

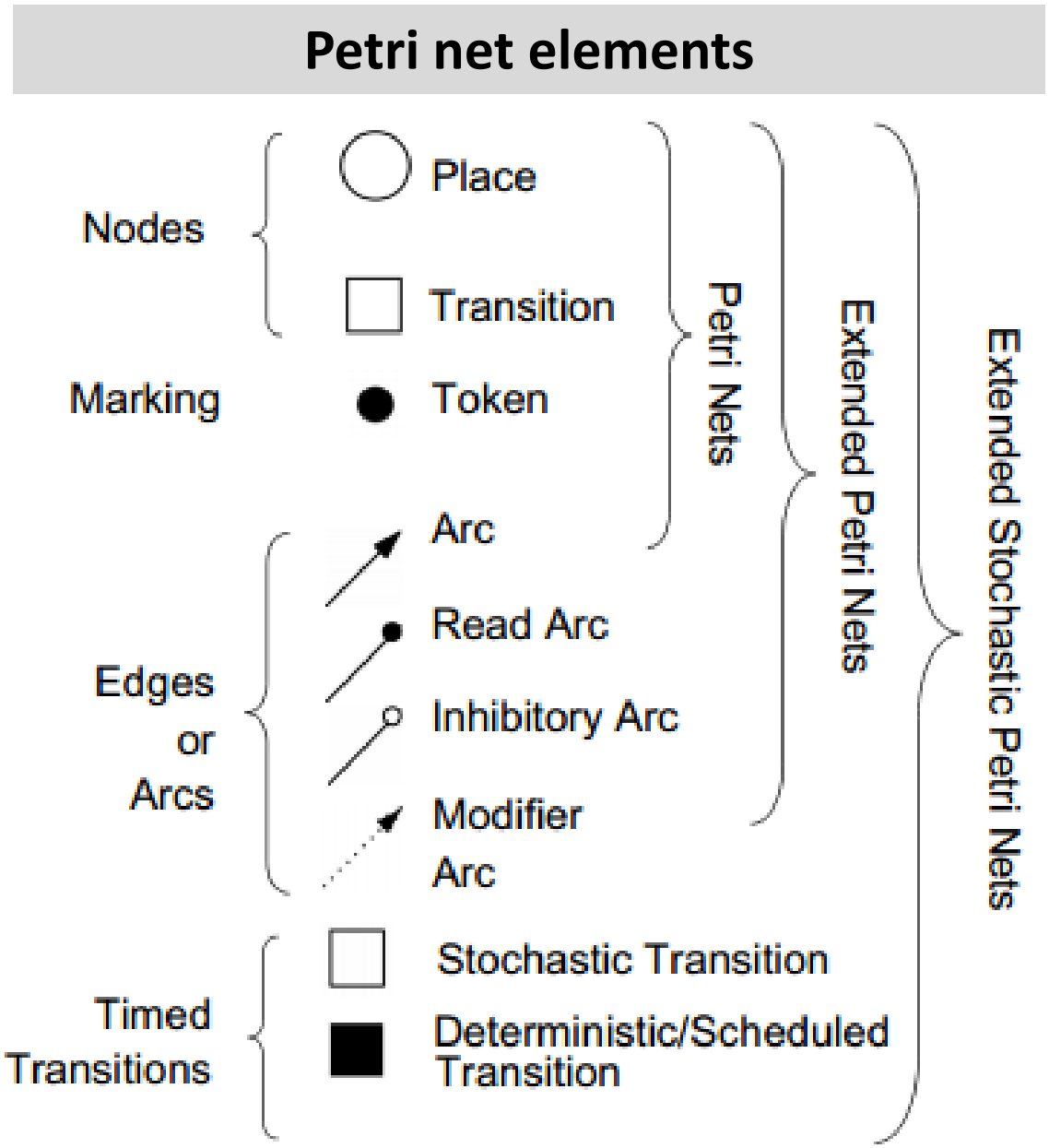

Figure 1: Petri net elements and their graphical representation. Petri nets are Weighted; directed; bipartite graphs consisting of nodes and arcs.

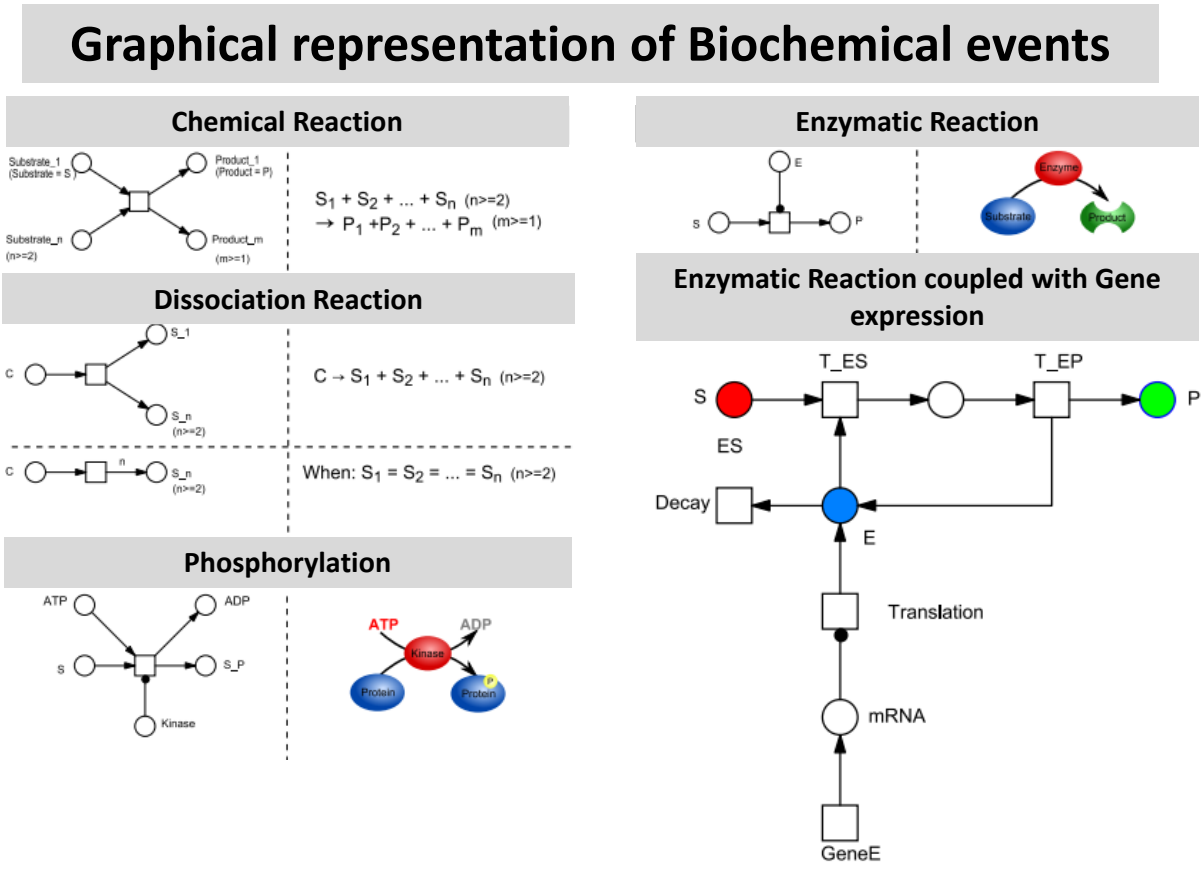

Figure 2: Graphical representation of Biochemical events using Petri-Net bipartite graph notation.

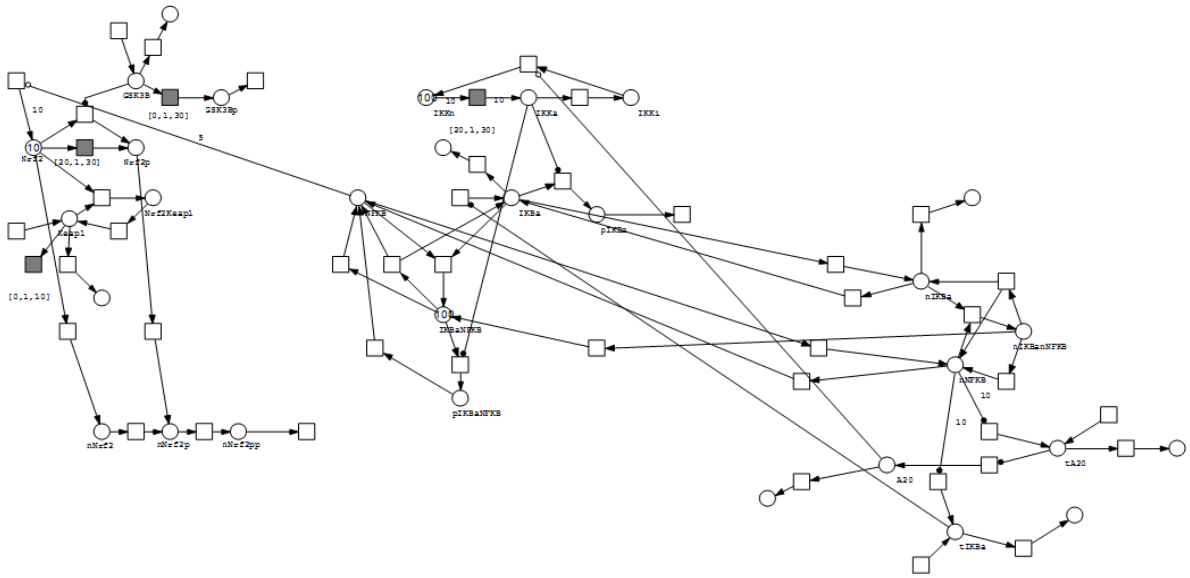

Figure 3: Bipartite graphic notation for both NFkB and Nrf2, this graphical notation is representative for variation number 5 which presented the most likely candidate for Asynchronous oscillations in the Cross-talk.

In order to simulate the results Snoopy can be used to simulate the token flow in the Petri-Net. Snoopy builds upon the Gillespie Algorithm, in this exact method a step-by-step simulation of possible states in the Petri-Net is performed. The standard simulation can be represented in 8 steps.

1. Initialise the Stochastic Petri-Net (SPN) network with the chosen initial marking
2. Calculate the firing rates of all enabled transitions using their rate functions
3. Calculate the combined rate by summing up all transition rates
4. Determine the time interval until the next state change takes place. This is done by computing an exponentially distributed random number
   depending on the current combined transition rate of the net (Figure 4)
5. Increase the simulation time by this time interval
6. Determine the next system state change. For this purpose, a
   weighted
   random selection of the transition is made which gets the license to fire
7. Let the selected transition fire and update the marking of the SPN
8. Go back to step 2, if the simulation time has not yet reached its end point

Each simulation run is one possible trace of the resultant token flow in the given interval. Therefore when doing Stochastic Petri-Nets multiple runs are required and then averaged to provide meaningful results.

In this Project an interval of 0-40 was used, with 100 output step counts at a refresh rate of 5000ms. 10 runs were done to give each trace in this Petri-Net.

.

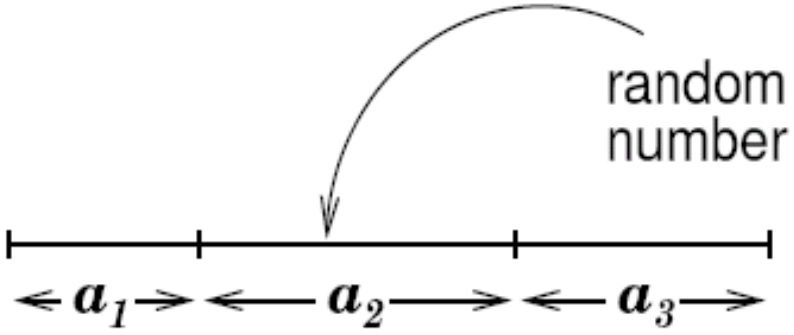

Figure 4 Random number associated and placement among weighted probability of firing (represented by size of a1;a2;a3)

Once the Simulation is completed and Token flow has been traced (e.g., Variant 1-6) Due to the difficulty in assessing whether nNFkB and nNrf2 oscillate in an asynchronous fashion, a graphical analysis was performed.

As it is illustrated in Figure 5, the presence of oscillations was observed as follows:
Both data traces, nNFkB(D1) and nNrf2(D2) had their average taken,

which followed by dividing every time point by the average minus one, thus providing a plot with positive or negative values in relation to the average. Once the positive and negative values for D1 and D2 were combined, all positive values were summed up (P) as were all negative values (n). Finally the Synchrony factor was obtained $F = \left(\frac{P}{P+n}\right)$: where P= positive values ; n= negative values. The final value was normalized to give a range from 0-1, with 0 representing perfect asynchronous behaviour, 0.5 perfectly random behaviour and a value of 1 being perfectly synchronous behaviour.

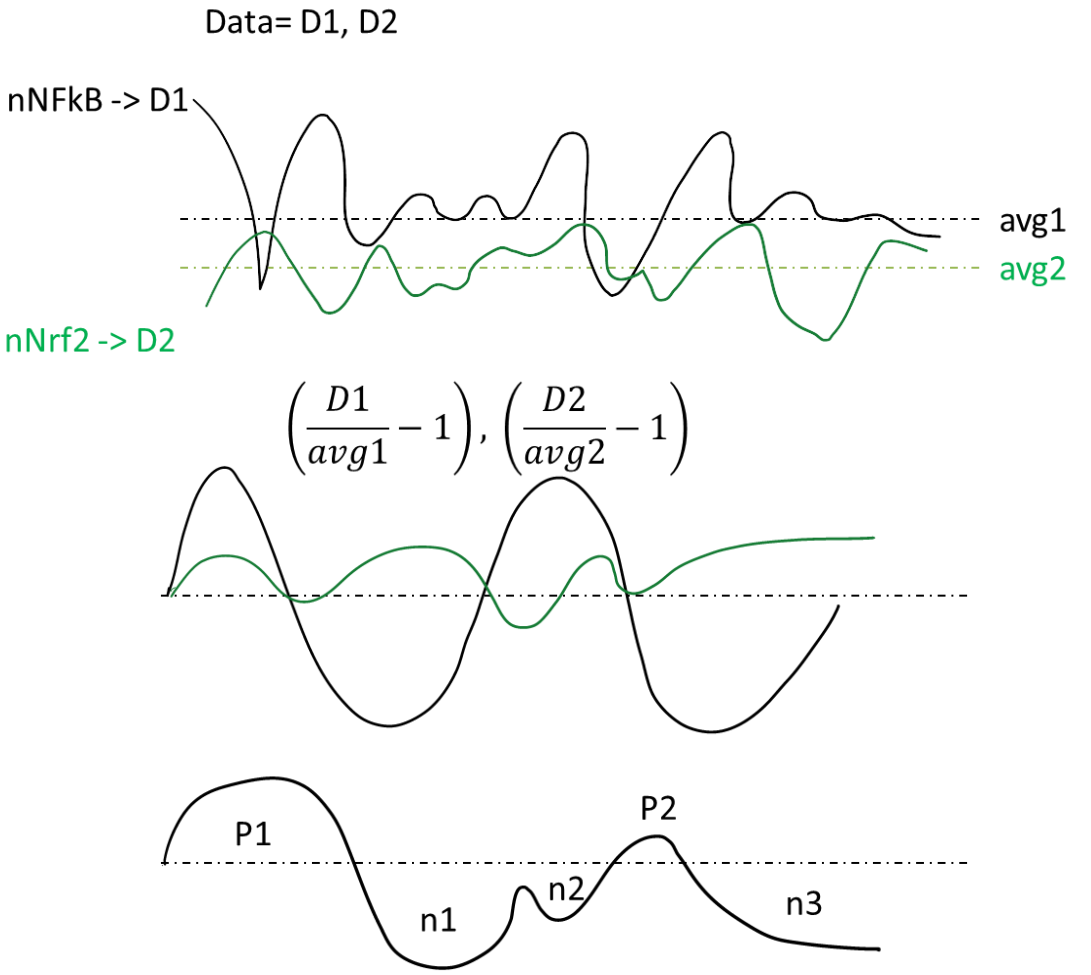

$$P = \sum Pi, \qquad SF = \frac{P}{P+n}$$

$$n = \sum ni \qquad SF: asynchronous \quad random \quad synchronous$$

$$0 \quad \rightarrow \quad 0.5 \quad \rightarrow \quad 1$$

Figure 5: Synchrony factor theoretical basis.

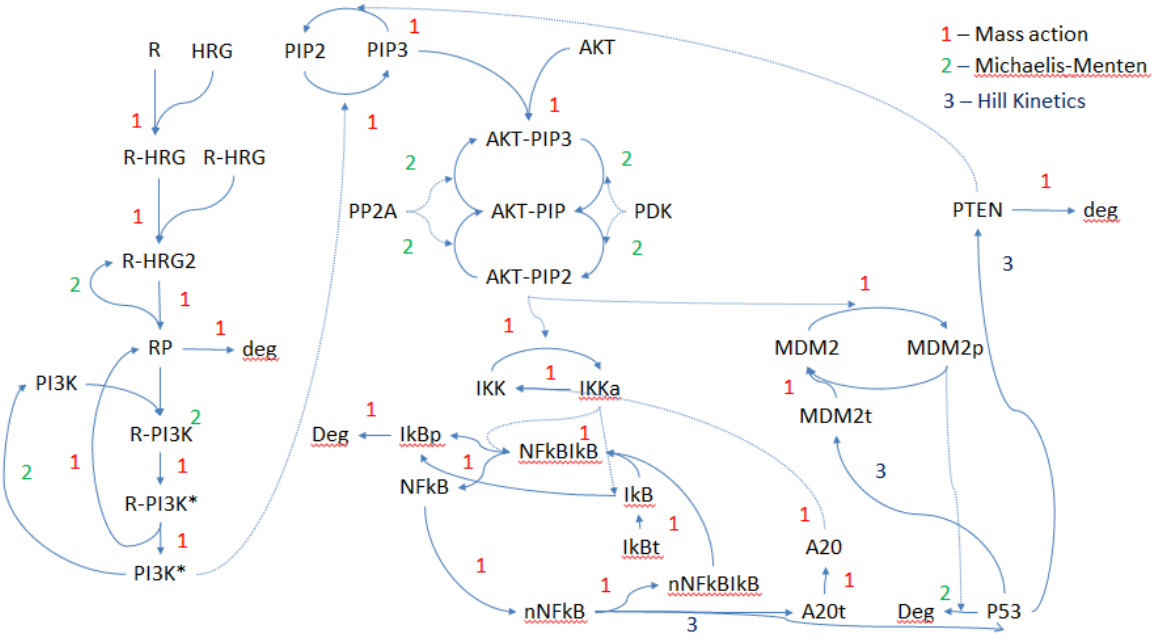

Figure 6: NFkB signal transduction pathway modelled in MATLAB using the ODE method. Use of either Mass Action, Hill Kinetics or Michaelis-Menten Kinetics is highlighted.

Results

The results for each simulation will be explained in this section for each one of the variants, with a trace representative of one simulation for each variant.

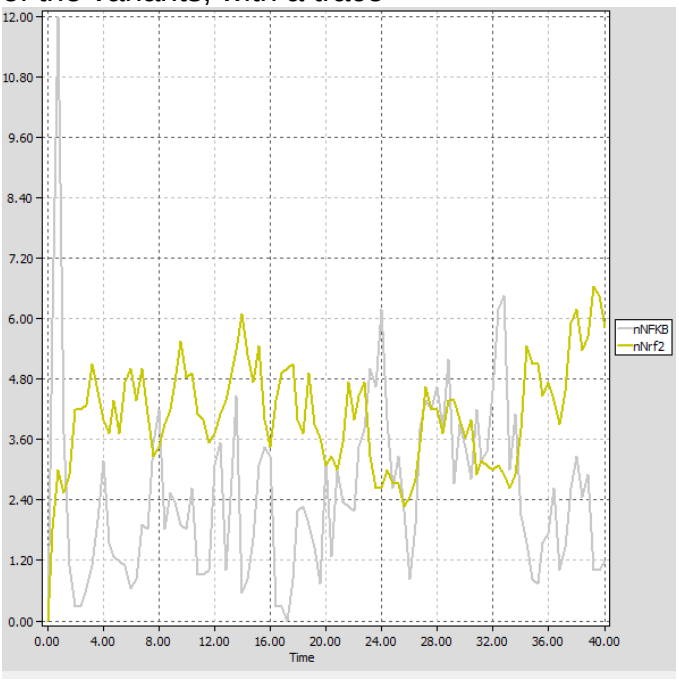

Variant 1 was used as a control, in this variant both NFkB and Nrf2 pathways were modelled independently, and ran through the simulations at the same time. They did not have any interaction points however.

Variant 1: Nrf2 and NFkB simulated independently

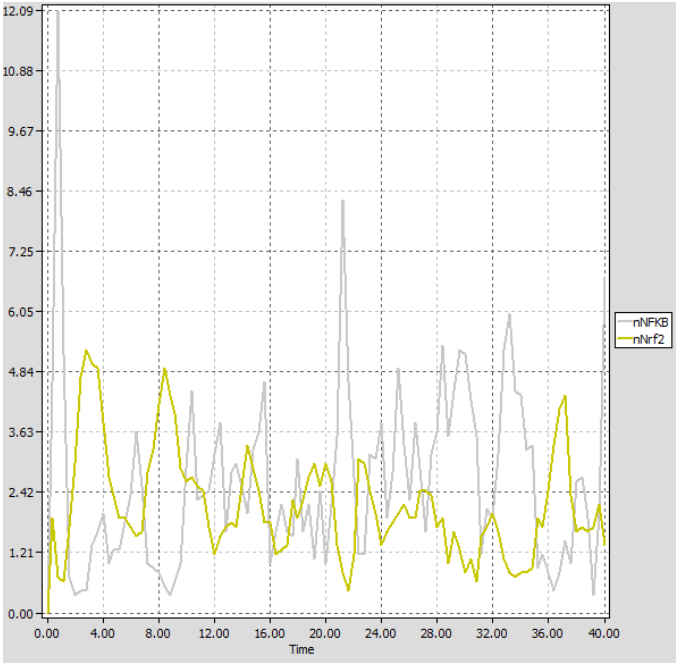

Variant 2 was based on the assumption that nuclear NFkB (nNFkB) through its activation of transcription factors would induce Gsk3B production in the nucleus this would lead to an increase in phosphorylated Nrf2, and thus reducing the amount bound to Keap1 that is primed for ubiquitination.

Variant 2: Nuclear NFkB induces GsK3B production in the nucleus

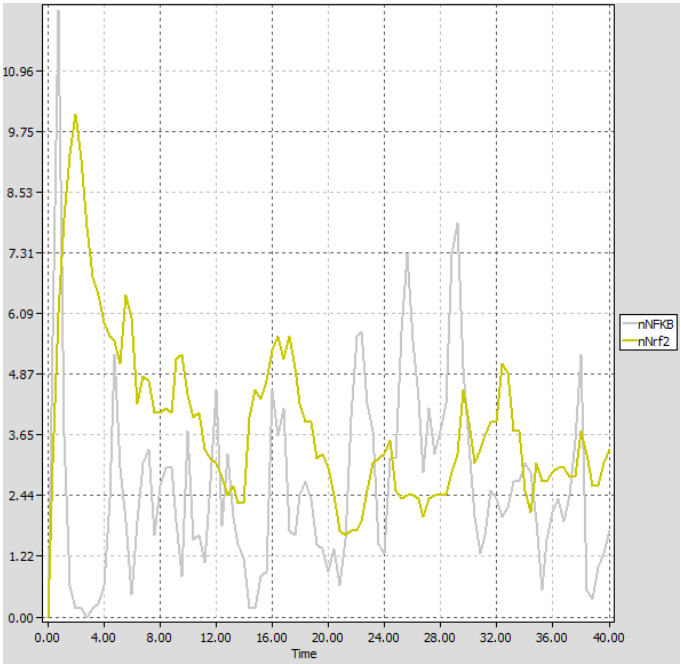

Variant 3 was based on the assumption that cytoplasmic NFkB (NFkB) would induce Keap1:Nrf2 binding in cytoplasm, not discriminating whether this would be because of increased synthesis, or facilitated interaction between Keap1 and Nrf2. .

Variant 3: Cytoplasmic NFkB induces Keap1:Nrf2 binding in cytoplasm

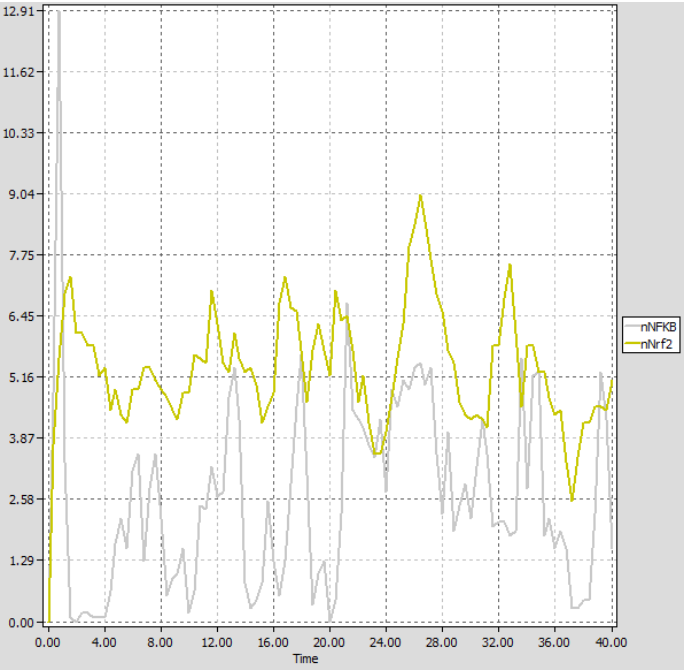

Variant 4 was based on the assumption that NFkB is able to de-phosphorylate Nrf2, thus allowing Nrf2 binding to Keap1 to occur.

Variant 4: Cytoplasmic NFkB induces de-phosphorylation of Nrf2 in cytoplasm

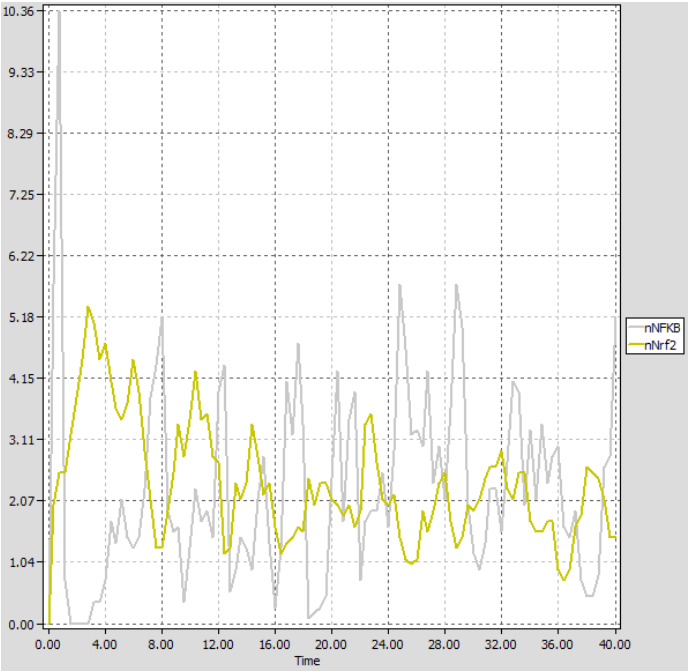

Variant 5 was based on the assumption that NFkB inhibits *de novo* synthesis of Nrf2 in cytoplasm thus decreasing overall free Nrf2 in the system.,

Variant 5: NFkB inhibits *de novo* synthesis of Nrf2 in cytoplasm

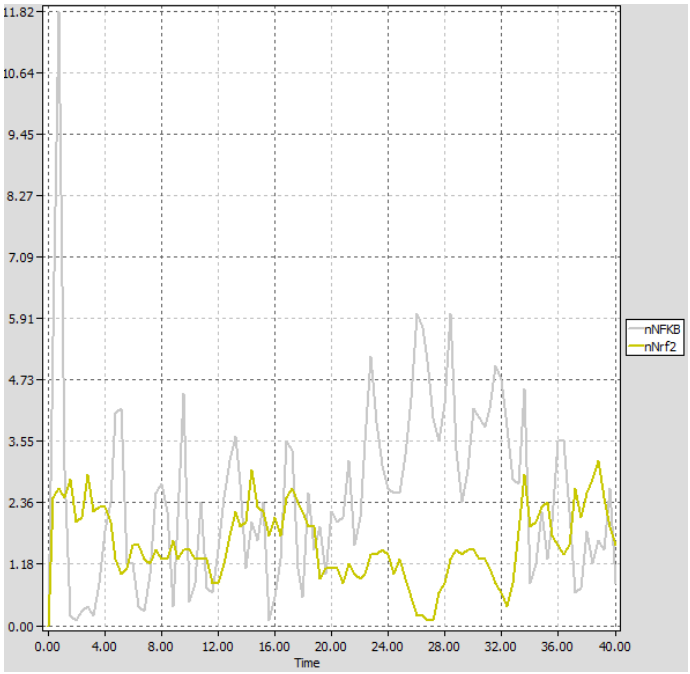

Variant 6 was a modified version of variant 5, it was based on the same assumption, however the *de novo* synthesis inhibition was set at a rate 20% that of Variant 5.

Variant 6: NFkB inhibits *de novo* synthesis of Nrf2 at 20% rate of variant 5

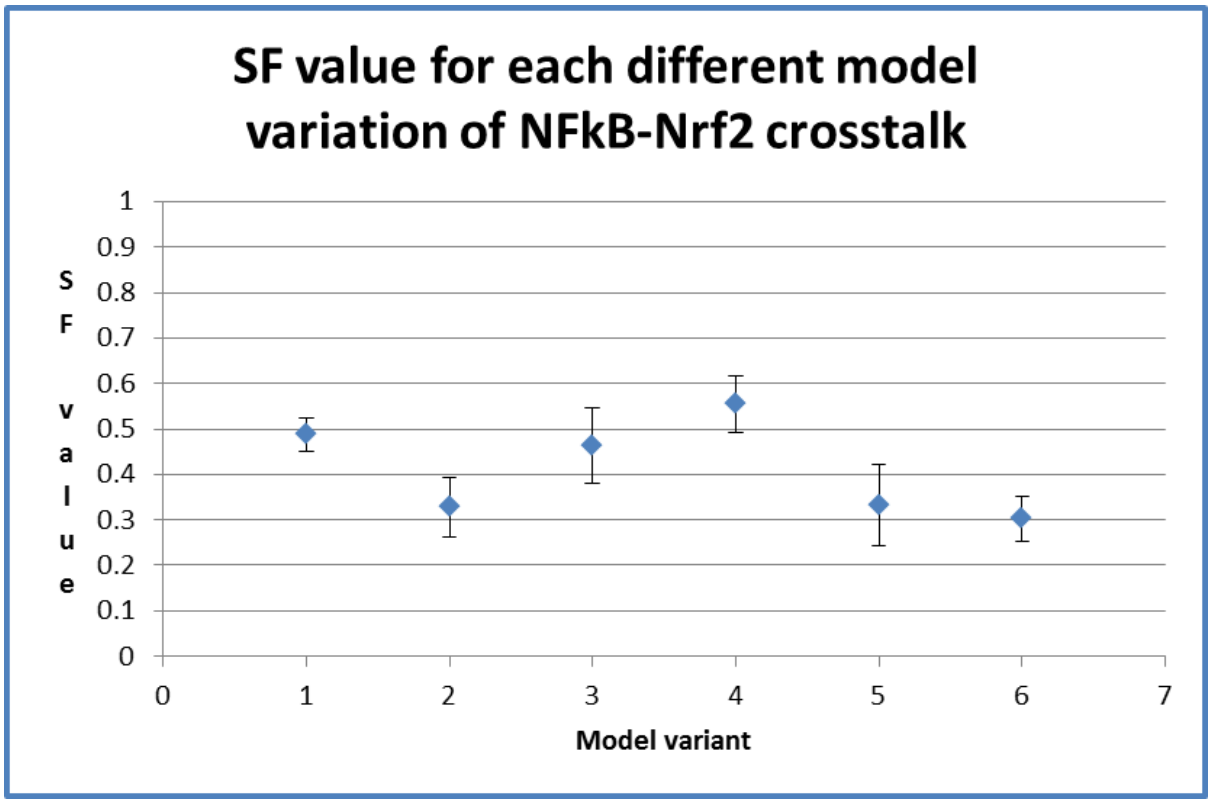

Figure 7: Synchrony factor in relation to each one of the NFkB-Nrf2 crosstalk models 0.5->1 synchronous behaviour ; 0.5->0 asynchronous behaviour ; 20 simulations each.

The simulations where then analysed, using the synchrony factor(SF) equation mentioned in the methods. For each variant, 20 simulations were

performed and their SF calculated, average taken and Standard deviation obtained for each variant, the results suggest that Variant 1, NFkB-Nrf2 independently have oscillations that are of a random nature. Variant 3 and 4 are also highly likely to be random, therefore they can be excluded as possible sources of asynchrony. Variant 2, 5 and, 6 however have shown to be the most likely candidates of asynchronous oscillations in NFkB-Nrf2 crosstalk, therefore GSk3B induction by NFkB and *de novo* synthesis inhibition of Nrf2 are two assumptions that should be studied further by experimentalists in order to identify the source of asynchronous oscillations.

Model validation:

In order to validate the Petri-Net model, a comparison with the ODE model for NFkB was done; given the non-parameterised, non-time dependent nature of this model the qualitative behaviour of the model was observed with more detail as opposed to its ability to accurately portray variation (in which ODE models have a clear advantage). In order to compare nNFkB and NFkB values were computed in the ODE (Figure 6) and Petri-Net (Figure 7) models, the main points are that the Petri-Net model has the correct behaviour, with an initial peak in NFkB which oscillates to give dampened oscillations, this was followed by nNFkB which oscillates to a slightly dampened state with a slight time delay in comparison, this is comparable to the behaviour of the ODE model.

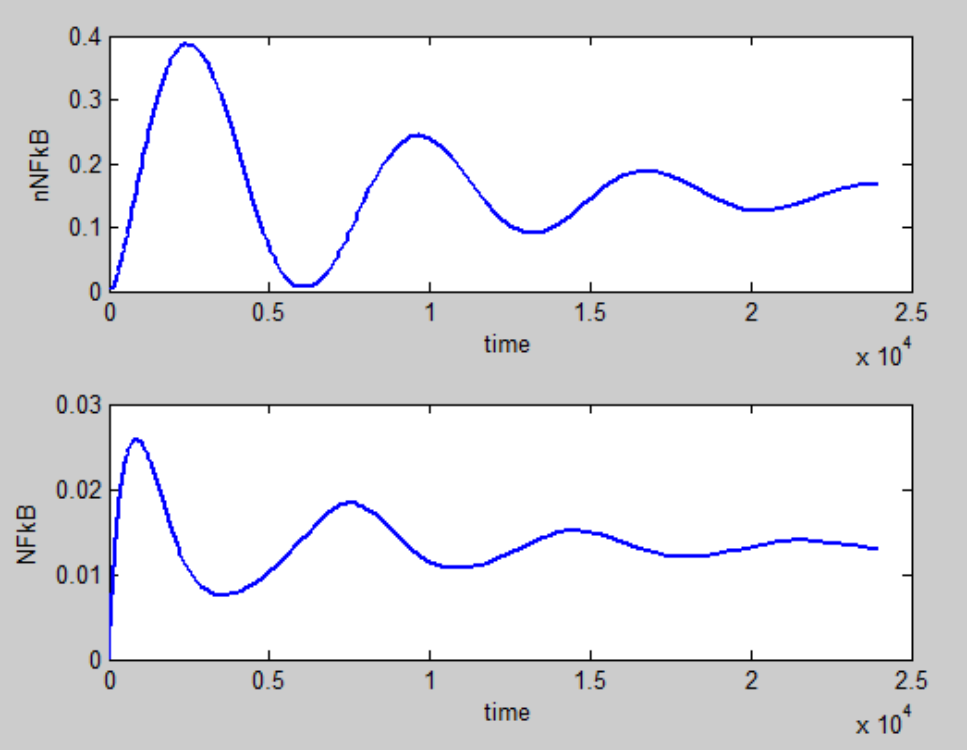

Figure 6: nNFkB and NFkB time course simulation based on ODE model using kinetic parameters

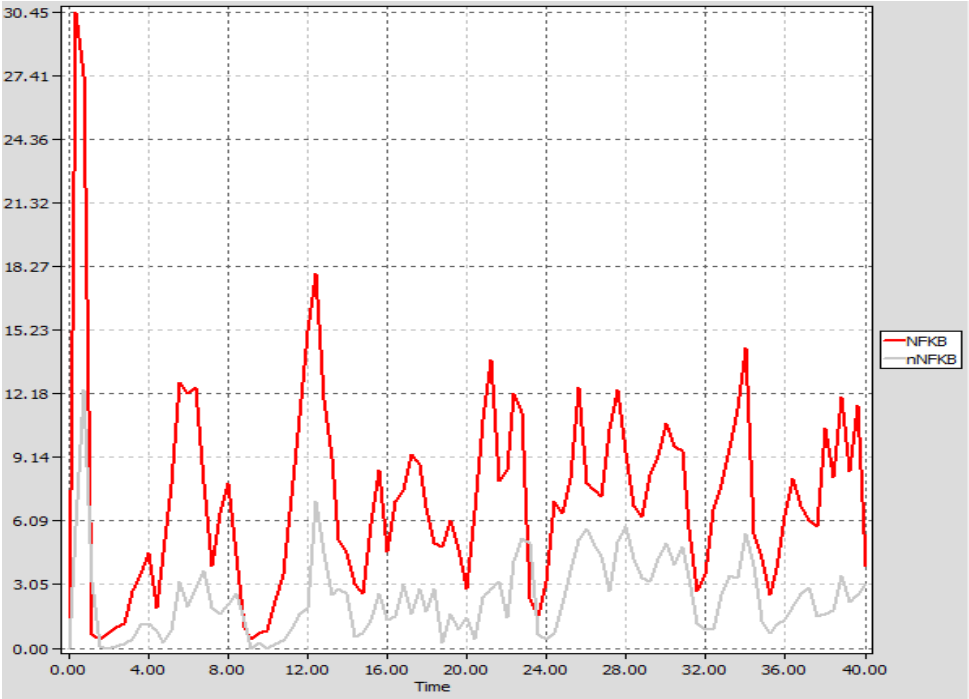

Figure 7: nNFkB and NFkB quantitative petri-net simulation showing delayed asynchronous oscillations(no kinetic parameters; not time dependent)

In order to validate the ODE model we aimed to match our time course profile with that of Total NFkB profile obtained through western blotting (1).

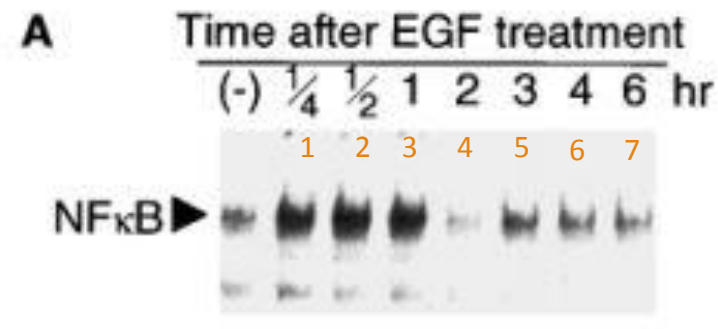

Figure 8: Western blot of a time course profile of Total NFkB for 6 hours (1)

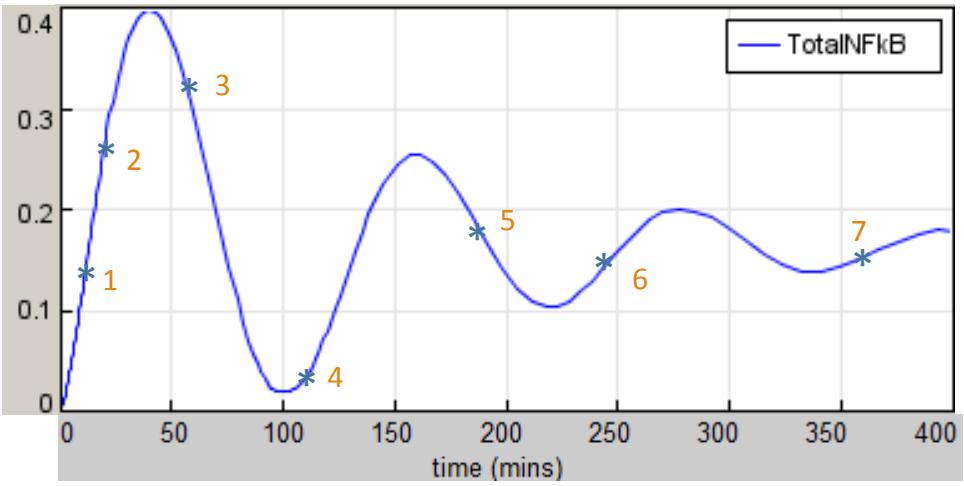

Figure 9: Time course simulation of the combined model of TotalNFkB for the duration of 400 minutes

The time course profile had similar behaviour to that seen in the western blot data, with an increase at ¼, ½ and, high TotalNFkB at 1 hour with a significant decrease by 2 hours and maintaining a relatively steady state through oscillations at 3, 4 and, 5 hours.

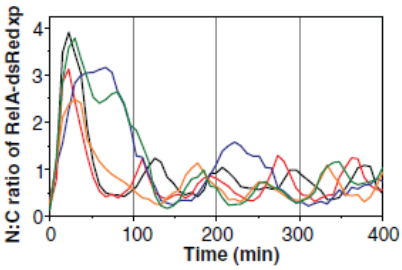

Figure 8 Nucleus to cytoplasm ratio of Rel A-dsRedxp as shown in the Ashall model (2)

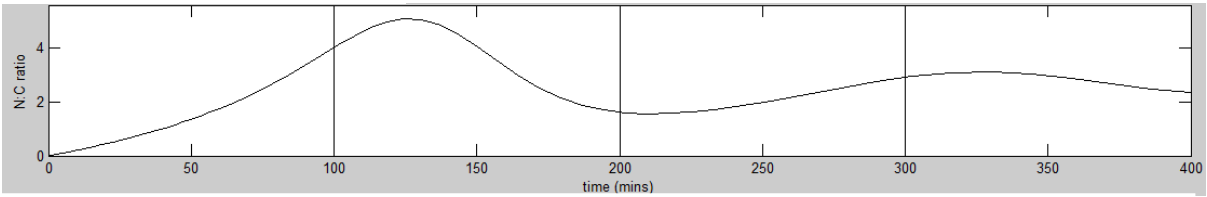

Figure 10: Nucleus to cytoplasm ratio of NFkB as obtained with the combined model.

For further validation we attempted to match the Nucleous:cytoplasm ratio presented in the Ashall model (2). The value obtained of 5 N:C ratio closely matched the N:C ratio peak of 4 shown in the Ashall model.

Discussion

At the end of this rotation, the use of Petri-Nets seems to be a valid approach to analyse signalling pathways where obtaining kinetic parameters would be experimentally unfeasible or too large to justify analysing each element of the pathway. However given the semi-quantitative nature of Petri-Nets in order to understand the Nrf2-NFkB crosstalk in a more meaningful way, it would be essential to obtain kinetic parameters for as many steps as viable for the Nrf2 pathway.

Conclusion

In its current state, the model is able to describe the oscillating behaviour of both NFkB and Nrf2, and given the assumptions taken, two of them seem to be appropriate candidates for further experimentation. Therefore in conclusion both *de novo* synthesis of Nrf2 inhibition by NFkB and Gsk3B induction by NFkB should be observed experimentally and time course profiles obtained for kinetic parameter extraction and further validation with an ODE model.

Acknowledgements

I would like to thank Dr Steven Webb and Dr Ian Sorrell for their continuing support during this rotation.

References

1. Ohtsubo M, Takayanagi A, Gamou S, Shimizu N. Interruption of NF kappa B-Stat1 signaling mediates EGF-induced cell-cycle arrest. J Cell Physiol. 2000;184(1):131-7.
2. Ashall L, Horton CA, Nelson DE, Paszek P, Harper CV, Sillitoe K, et al. Pulsatile Stimulation Determines Timing and Specificity of NF-kappa B-Dependent Transcription. Science. 2009;324(5924):242-6.
3. Ghosh S, Karin M. Missing pieces in the NF-kappaB puzzle. Cell. 2002;109 Suppl:S81-96.
4. Oeckinghaus A, Hayden MS, Ghosh S. Crosstalk in NF-kappaB signaling pathways. Nat Immunol. 2011;12(8):695-708.
5. Lin A, Karin M. NF-kappaB in cancer: a marked target. Seminars in cancer biology. 2003;13(2):107-14.
6. Advani RH, Buggy JJ, Sharman JP, Smith SM, Boyd TE, Grant B, et al. Bruton tyrosine kinase inhibitor ibrutinib (PCI-32765) has significant activity in patients with relapsed/refractory B-cell malignancies. Journal of clinical oncology : official journal of the American Society of Clinical Oncology. 2013;31(1):88-94.
7. Senior K. Positive results for ibrutinib in B-cell malignancies. Lancet Oncol. 2012;13(12):E522-E.
8. Basak S, Hoffmann A. Crosstalk via the NF-kappaB signaling system. Cytokine & growth factor reviews. 2008;19(3-4):187-97.
9. Kurzrock R, Estrov Z, Ku S, Leonard M, Talpaz M. Interleukin-1 increases expression of the LYT-10 (NFkappaB2) proto-oncogene/transcription factor in renal cell carcinoma lines. The Journal of laboratory and clinical medicine. 1998;131(3):261-8.
10. Lipniacki T, Paszek P, Brasier AR, Luxon B, Kimmel M. Mathematical model of NF-kappaB regulatory module. Journal of theoretical biology. 2004;228(2):195-215.
11. Marwan W, Rohr C, Heiner M. Petri nets in Snoopy: a unifying framework for the graphical display, computational modelling, and simulation of bacterial regulatory networks. Methods in molecular biology. 2012;804:409-37.
12. Hardy S, Robillard PN. Modeling and simulation of molecular biology systems using petri nets: modeling goals of various approaches. Journal of bioinformatics and computational biology. 2004;2(4):595-613.
13. Hatakeyama M, Kimura S, Naka T, Kawasaki T, Yumoto N, Ichikawa M, et al. A computational model on the modulation of mitogen-activated protein kinase (MAPK) and Akt pathways in heregulin-induced ErbB signalling. The Biochemical journal. 2003;373(Pt 2):451-63.
14. Gong HJ, Zuliani P, Komuravelli A, Faeder JR, Clarke EM. Analysis and verification of the HMGB1 signaling pathway. Bmc Bioinformatics. 2010;11.
15. Michaelis L, Menten ML. The kinetics of the inversion effect. Biochem Z. 1913;49:333-69.
16. Briggs GE, Haldane JB. A Note on the Kinetics of Enzyme Action. The Biochemical journal. 1925;19(2):338-9.
17. Barcroft J, Hill AV. The nature of oxyhaemoglobin, with a note on its molecular weight. The Journal of physiology. 1910;39(6):411-28.
18. Rossi FM, Kringstein AM, Spicher A, Guicherit OM, Blau HM. Transcriptional control: rheostat converted to on/off switch. Molecular cell. 2000;6(3):723-8.
19. Alon U. An introduction to systems biology : design principles of biological circuits. Boca Raton, Fla. ; London: Chapman & Hall/CRC; 2006. xvi, 301 p. p.
20. Ferrell JE, Jr., Machleder EM. The biochemical basis of an all-or-none cell fate switch in Xenopus oocytes. Science. 1998;280(5365):895-8.
21. Holt JM, Ackers GK. The Hill Coefficient: Inadequate Resolution of Cooperativity in Human Hemoglobin. Method Enzymol. 2009;455:193-212.
22. Krebs JE. Lewin's genes XI. 11th / edited by Jocelyn E. Krebs, Stephen T. Kilpatrick, Elliott S. Goldstein. ed. Sudbury, Mass.: Jones and Bartlett; 2013. xxvii, 940 p p.

Annex

Combined model (2, 10, 13, 14) –

Table 5 Description of the final combined model for the NFkB pathway. Highlighted in red are parameters modified based on sensitivity analysis.

	Parameter Values	Units	Reaction description	Type of Reaction	Reaction kinetics
1f	0.0012*10^-3	1/(uM*s)	R + HRG -> R-HRG	Mass Action	k1*[ErbB4-R]*HRG
1r	0.00076 ; 1/s	1/s	R-HRG -> R + HRG	Mass Action	[k1']*R_HRG
2f	0.01*10^-3 ; 1/(uM*s)	1/(uM*s)	R-HRG -> R-HRG2	Mass Action	k2*R_HRG^2
2r	0.1 ; 1/s	1/s	R-HRG2 -> R-HRG	Mass Action	[k'2]*R_HRG2
3f	1 ; 1/s	1/s	R-HRG2 -> RP	Mass Action	k3*R_HRG2
3r	0.01 ; 1/s	1/s	RP -> R-HRG2	Mass Action	[k3']*RP
4f	V4= 62.5 *10^-3 ; 1/(uM*s) ; K4= *10^-3 ; uM	V4= 1/(uM*s) K4= uM	RP -> R-HRG2	Michaelis-Menten	V4*RP/(K4+RP)
5f	0.001 ; 1/s	1/s	RP -> null	Mass Action	k34*RP
6f	0.1*10^-3 ; 1/(uM*s)	1/(uM*s)	PI3K + RP -> R-PI3K	Mass Action	k23*PI3K*RP
6r	2 ; 1/s	1/s	R-PI3K -> PI3K + RP	Mass Action	[k23']*R_PI3K
7f	9.85 ; 1/s	1/s	R-PI3K -> R-PI3K*	Mass Action	k24*R_PI3K
7r	0.0985 ; 1/s	1/s	R-PI3K* -> R-PI3K	Mass Action	[k24']*[R_PI3K*]
8f	45.8 ; 1/s	1/s	R-PI3K* -> RP + PI3K*	Mass Action	k25*[R_PI3K*]
8r	0.047 *10^-3 ; 1/(uM*s)	1/(uM*s)	RP + PI3K* -> R-PI3K*	Michaelis-Menten	[k25']*[PI3K*]*RP
9f	V26= 2620 *10^-3 ; 1/(uM*s) ; K26= 3680 *10^-3 ; uM	V26= 1/(uM*s) ; K26= uM	PI3K* -> PI3K	Michaelis-Menten	V26*[PI3K*]/(K26+[PI3K*])
10f	0.000003 ; 1/molecule*minute V 3e-6*cscale*(60* 10^-3) =225 *10^-3 ; 1/(uM*s)	1/(uM*s)	PI3K* induces PIP2 -> PIP3	Mass Action	k3*PI3Ka*PIP2

10r	k27=16.9 *10^-3 ; 1/(uM*s) ; K27=39.1 ; 1/s	k27= 1/(uM*s) K27=1/s	PI3K* induces PIP2 -> PIP3	Michael is-Menten	(k27*[PI3K*]*PI)/(K27+PI)
11f	507*10^-3 ; 1/(uM*s)	1/(uM*s)	PIP3 + AKT -> AKT-PIP3	Mass Action	k29*PIP3*AKT
11r	234 ; 1/s	1/s	AKT-PIP3 -> PIP3 + AKT	Mass Action	k_29*AKT_PIP3
12f	V30=20000 *10^-3 ; 1/(uM*s) ;K30=80000* 10^-3 ; uM	V30=1/(uM*s) K3-1/(uM*s)	PDK induces AKT-PIP3 -> AKT- PIP	Michael is-Menten	(V30*AKT_PIP3)/(K30+AKT_PIP3)
13f	k3 1=0.107; 1/s ;K31=4.35 *10^-3 ; uM	k31= 1/s K31= uM	P P2A induces AKT-PIP -> AKT-PIP3	Michael is-Menten	(k31*PP2A*AKT_PIP)/(K31+AKT_ PIP3)
14f	V32=20000*1 0^-3 ; 1/(uM*s) ;K32=80000 *10^-3 ; uM	V32= 1/(uM*s) K32= uM	PDK induces AKT-PIP -> AKT-PIP2	Michael is-Menten	(V32*AKT_PIP)/(K32+AKT_PIP)
15f	k33=0.211; 1/s K33=12*10^-3 ; uM	k33= 1/s K33= uM	PP2A induces AKT-PIP2 -> AKT-PIP	Michael is-Menten	(k31*PP2A*AKT_PIP)/(K31+AKT_ PIP3)
16f	2.50E-03	1/(uM*s)	AKT-PIP2 activates IKKn -> IKKa	Mass Action	k1*Cytoplasm.IKKn*Cytoplasm.AK T_PIP2
17f	1.25E-04	1/s	IKKn -> deg2	Mass Action	k2*Cytoplasm.IKKn
18f	k4= 0.1 ; k5g=0.064	k4= 1/(uM*s) ; k5g= uM	IKKa + A20 -> IKKi + A20	Mass Action	k5*Cytoplasm.IKKa+k4*Cytoplas m.IKKa*Cytoplasm.A20
19f	1.25E-04	1/s	IKKi -> deg	Mass Action	k11*Cytoplasm.IKKi
20f	0.2	1/(uM*s)	IkBa + IKKa -> IKKa_IkBa	Mass Action	k7*Cytoplasm.IKKa*Cytoplasm.Ik Ba
21f	0.1	1/s	IKKa_IkBa -> IKKa	Mass Action	k8*Cytoplasm.IKKa_IkBa
22f	1.25E-04	1/s	IKKa -> deg	Mass Action	k6*Cytoplasm.IKKa
23f	5.3E-4	1/s	(IKKa Induced)NFk B_IkBa + IKKa -> NFkB + IKKa	Mass Action	k12*Cytoplasm.NFkB_IkBa
24f	0.1	1/s	NFkB_IkBa_I KKa -> NFkB + IKKa	Mass Action	k10*Cytoplasm.NFkB_IkBa_IKKa
25f	1	1/(uM*s)	IKKa + NFkB_IkBa -	Mass Action	k9*Cytoplasm.IKKa*Cytoplasm.NF kB_IkBa

			> NFkB_IkBa_IKKa		
26f	18.4	1/(uM*s)	IkBa + NFkB -> NFkB_IkBa	Mass Action	kf13*Cytoplasm.NFkB*Cytoplasm.IkBa
26r	18.4	1/s	NFkB_IkBa -> IkBa + NFkB	Mass Action	kr13*Cytoplasm.NFkB_IkBa
27f	1.00E-04	1/s	IkBa -> deg	Mass Action	k21*Cytoplasm.IkBa
28f	0.001	1/s	IkBa -> 5 nIkBa	Mass Action	kf23*Cytoplasm.IkBa
28r	5.00E-04	1/s	5 nIkBa -> IkBa	Mass Action	kr23*nucleus.nIkBa
29f	0.0025	1/s	NFkB -> 5 nNFkB	Mass Action	kf15*Cytoplasm.NFkB
29r	0	1/s	5 nNFkB -> NFkB	Mass Action	kr15*nucleus.nNFkB
30f	18.4	1/(uM*s)	nNFkB + nIkBa -> nNFkB_nIkBa	Mass Action	kf14*nucleus.nNFkB*nucleus.nIkBa
30r	0	1/s	nNFkB_nIkBa -> nNFkB + nIkBa	Mass Action	kr14*nucleus.nNFkB_nIkBa
31f	0.01	1/s	5 nNFkB_nIkBa -> NFkB_IkBa	Mass Action	kf28*nucleus.nNFkB_nIkBa
31r	0	1/s	NFkB_IkBa -> 5 nNFkB_nIkBa	Mass Action	kr28*Cytoplasm.NFkB_IkBa
32f	3.4E-7	1/s	nNFkB + nIkBa -> mRNAIkBa + nNFkB	Mass Action	k26*nucleus.nNFkB
33f	4.00E-04	1/s	mRNAA20 -> deg	Mass Action	k17*Cytoplasm.mRNAA20
34f	0.5	1/s	mRNAA20 -> A20 + mRNAA20	Mass Action	k16*Cytoplasm.mRNAA20
35f	3.00E-04	1/s	A20 -> deg	Mass Action	k18*Cytoplasm.A20
36f	4.00E-04	1/s	mRNAIkBa -> deg	Mass Action	k27*Cytoplasm.mRNAIkBa
37f	0.5	1/s	mRNAIkBa -> IkBa + mRNAIkBa	Mass Action	k22*Cytoplasm.mRNAIkBa
38f	kp= 6.0E-4 ; kbA20= 0.0018	kp= uM^2/s ; kbA20= uM/s	IKKi -> IKKn	Mass Action	kp*IKKi*(kbA20/(kbA20+Cytoplasm.A20*AKT_PIP2))
39f	k5g=0.064 K1=0.016	k5g= 1/s ; K1=1/(u	null -> PTEN	Hill Kinetics	k5g*Cytoplasm.P53^3/(K1^3+Cytoplasm.P53^3)

		M*s)			
40f	0.006	1/s	PTEN -> null	Mass Action	d5*Cytoplasm.PTEN
41f	k9g= 9.6E-7 ; kp=4.0E-15 ; Kn=0.04	k9g= uM/s ; kp= uM/s ; Kn= uM	nNFkB -> .P53 + nNFkB	Michaelis-Menten	k9g+k9p*nucleus.nNFkB/(Kn+nucleus.nNFkB)
42f	d9p=6.0E-7 ; d9= 0.012	d9p= uM/s ; d9= 1/s	P53 -> null	Michaelis-Menten	(d9+d9p*Cytoplasm.MDM2p)*Cytoplasm.P53
43f	k6g=4.267E-7 ; K1g=0.064	k6g= uM/s ; K1g= uM	P53 -> MDM2t + P53	Hill Kinetics	k6g*Cytoplasm.P53^3/(K1g^3+Cytoplasm.P53^3)
44f	0.018	1/s	MDM2t -> null	Mass Action	d6*Cytoplasm.MDM2t
45f	0.5	1/s	MDM2t -> MDM2 + MDM2t	Mass Action	k7g*Cytoplasm.MDM2t
46f	2.33E-04	1/s	MDM2 -> null	Mass Action	d7*Cytoplasm.MDM2
47f	k8g=3.2E-13 ; d8= 5.0E-4	k8g= 1/(uM*s) ; d8= 1/s	MDM2 -> MDM2p	Mass Action	k8g*Cytoplasm.AKT_PIP2*Cytoplasm.MDM2
48f	5.0E-4	1/s	MDM2p -> MDM2	Mass Action	d8*Cytoplasm.MDM2p
48r	2.17E-04	1/s	MDM2p -> null	Mass Action	d8p*Cytoplasm.MDM2p

All do the models shown were then combined into a composite model of NFkB signalling, linking the Hatakeyama model through PIP2 phosphorylation, Akt_pip3 part of the pathway being used as a TNF-alpha analogue to mediate IKK activation whilst also interacting with the MDM2 phosphorylation step, The neutral state was added from the Ashall model and from the Lipniacky model a increased feedback generated by increased transcription of P53.

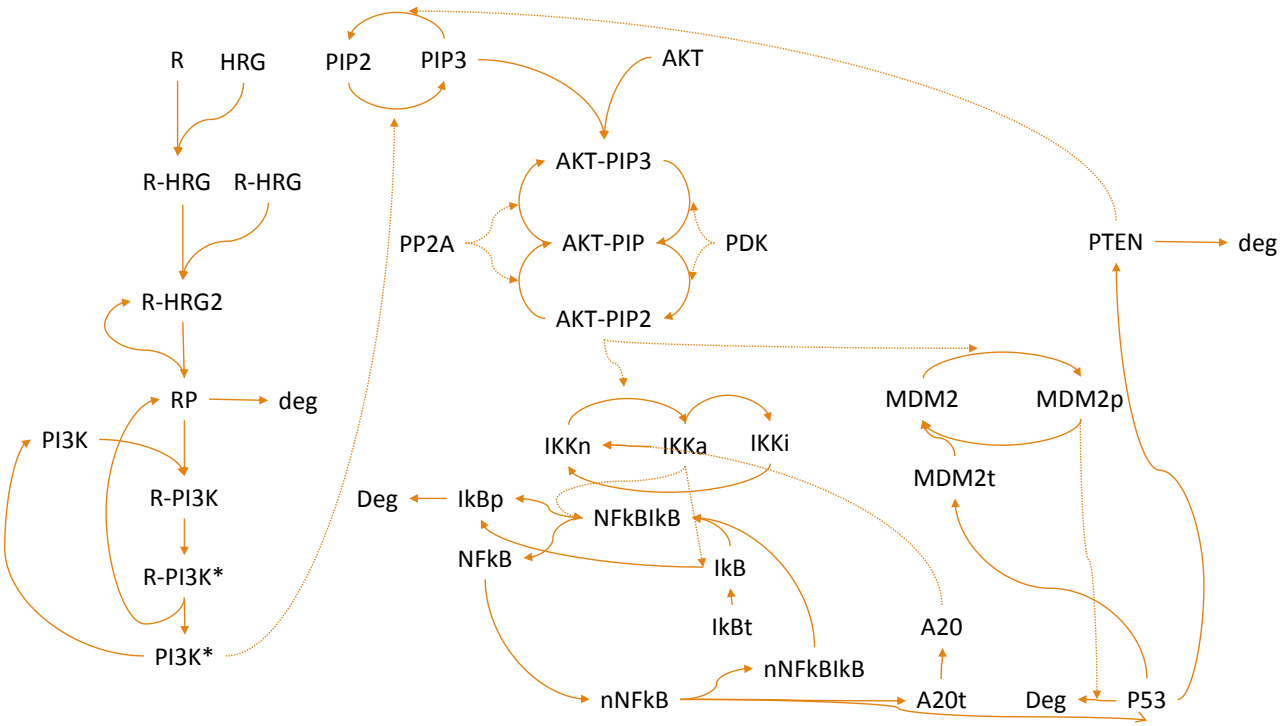

Figure 5 Diagrammatic representation of the combined model of the NFkB pathway.

Initial conditions

Table 6 Initial conditions for the simulation of the Combined model

Species	Value	Units
NFkB_IkBa	0.16	µM
ErbB4_R	0.08	µM
HRG	0.01	µM
PI3K_1	0.01	µM
AKT	0.01	µM
PP2A	1.14E-5	µM
PIP2	0.08	µM
MDM2t	0.0080	µM
MDM2p	0.016	µM
P53	0.016	µM
MDM2	0.0080	µM

Kinetic laws:

Mass action- The law of mass action states that the reaction rate is proportional to the probability of a collision of the reactants, which is in turn proportional to the concentration of the reactants.

Assuming a reversible reaction of two substrates S_1 and S_2

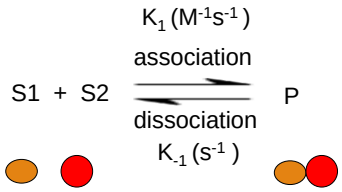

The net reaction rate is given by the rate of the forward reaction minus the rate of the backward reaction:

$$\frac{d[P]}{dt} = -\frac{d[S_1]}{dt} = -\frac{d[S_2]}{dt} = k_1[S_1][S_2] - k_{-1}[P]$$

In which k_1 and k_{-1} are kinetic, or rate, constants and, [.] denotes concentration.

Michaelis-Menten kinetics- First described by Leonor Michaelis and Maud Menten (15)

Michaelis-Menten equation for an isolated reaction:

$S \xrightarrow{E} P$: Substrate S is transformed into product P through a catalysed reaction using enzyme E (where S can be a inactive/dephosphorylated form of a protein, P can be an activated/phosphorylated form of the protein and E is the enzyme or kinase catalysing the reaction). For an isolated system, the rate of production of P (dP/dt) is proportional to the rate of consumption of S (dS/dt) and therefore the rate of reaction (v) can be written as follows:

$$v = \frac{d[P]}{dt} = -\frac{d[S]}{dt} = \frac{V_{max}[S]}{K_M + [S]}$$

Where K_M (µM) is the Michaelis-Menten dissociation constant and V_{max} (1/s) is the maximum velocity rate. A full derivation of this formula can be expressed as follows. Consider the following enzyme-substrate reaction.

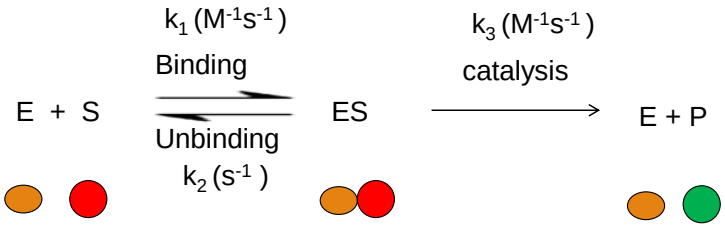

Then, according to the Law of Mass Action, we have

$$\frac{d[E]}{dt} = -k1[E][S] + k3[ES] + k2[ES]$$

$$\frac{d[ES]}{dt} = k1[E][S] - k2[ES] - k3[ES]$$

and

$$\frac{d[P]}{dt} = k3[ES]$$

A quasi-steady state assumption is then assumed. This quasi steady state assumption was first stipulated by Briggs and Haldane in 1925 (16) and assumes the following:

$$\frac{dES}{dt} = 0 = \frac{dE}{dt}$$

Therefore:

$$0 = +k1[E][S] - k3[ES] - k2[ES]$$

With a constant number of enzyme

$$[E]_0 = [E] + [ES]$$

This becomes

$$0 = k1([E]_0 - [ES])[S] - (k2 + k3)[ES]$$

Rearranging for [ES] gives

$$[ES] = \frac{[E]_0[S]}{\frac{k2 + k3}{k1} + [S]}$$

Substituting into the d[p]/d[t] equation then gives

$\frac{d[P]}{dt} = \frac{(k3[E]_0)[S]}{[S]+K_M}$ Where $(k3[E]_0) = Vmax$

Namely

$$\frac{d[P]}{dt} = \frac{Vmax[S]}{[S]+K_M}$$

Hill kinetics: First proposed by Barcroft and Hill (17) in order to explain how haemoglobin O_2 saturation curves generated a sigmoidal curve and proposed the use of an exponential power to produce the sigmoidal curve with theoretical basis on multiple subunit binding.

Various molecular mechanisms have been stated to explain the sigmoidal curves generated with Hill kinetics, which often are representative of biomolecular processes such as transcription(18, 19). Molecular mechanisms that have been stipulated in order to explain this behaviour include: cooperative binding sites (17) multimer formation(19), competition between a repressor and an activator on a given binding site (18) and positive-feedback loop models (20).Sigmoid responses are therefore mostly seen in multimeric systems with cooperative interactions. Binding at one site results in a change in the binding affinities of the remaining sites and therefore Hill kinetics can present limitations when assessing relative contributions of each cooperative molecule (21).

Hill equation derivation-

Assume that an enzyme (E) binds, for example, simultaneously with multiple (n) substrates (S), namely:

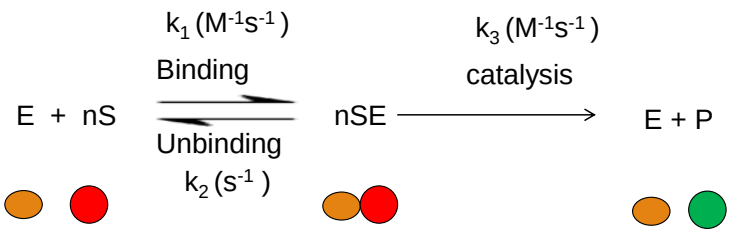

Following the same quasi-steady state argument stipulated by Briggs and Haldane (16), namely that d[nSE]/dt=0 , and again assuming a constant number of enzyme ($[E]_0$), one can obtain

$$\frac{d[P]}{dt} = \frac{(k_3[E]_0 S^n)}{\frac{k_2 + k_3}{k_1} + S^n} = \frac{Vmax + S^n}{K_M + S^n}$$

Where n is often described as the Hill coefficient.

In order to improve the mathematical model besides the wet lab parameter estimation, different approaches to modelling could be used to improve the current model. As an alternative to using the Hill equation, Sequential binding could be used, thus allowing the addition of effectors and therefore transcriptional repressors or activators for the P53 and A20 modules in the model. Limitations of Michaelis-Menten kinetics also affect the validity of the model, as it is derived for isolated enzyme reactions. It raises issues of whether it remains sufficiently valid when extrapolated into a large reaction network or a multiple cell system. In natural conditions, steady state is not the norm and the reactants may be affected my perturbations or oscillatory inductions. Further issues arise when describing processes such as mRNA transcription since Hill kinetics and Michaelis-Menten kinetics were derived in the context of enzymatic reactions. This is because gene transcription is a multi-step process that utilizes molecular machinery at multiple levels (22).

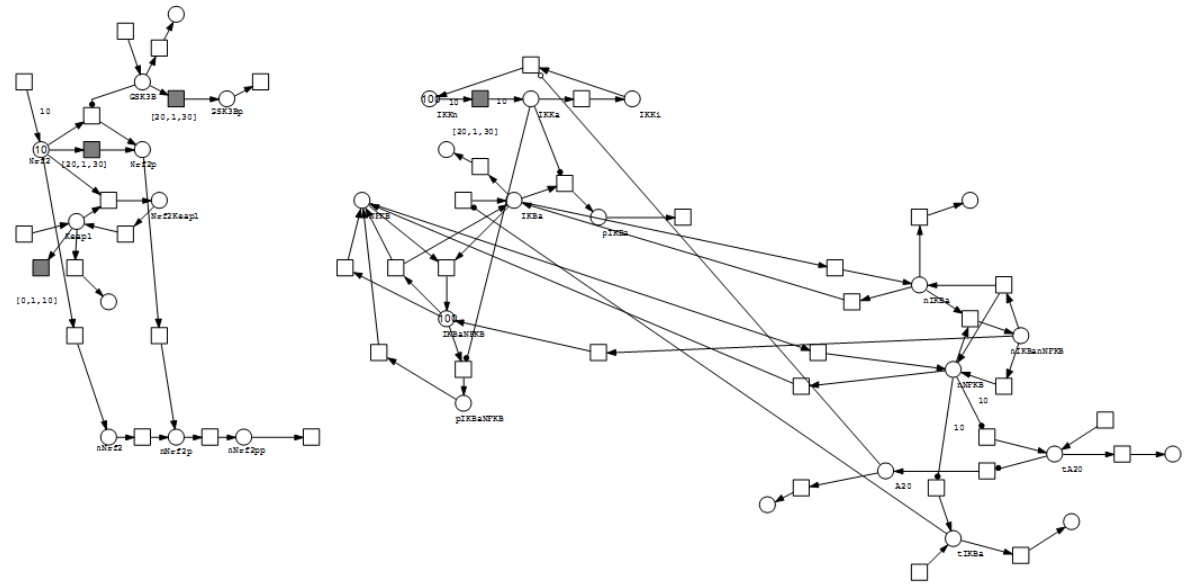

Figure 1: Bipartite graphic notation for both NFkB and Nrf2, this graphical notation is representative for variation number 1.

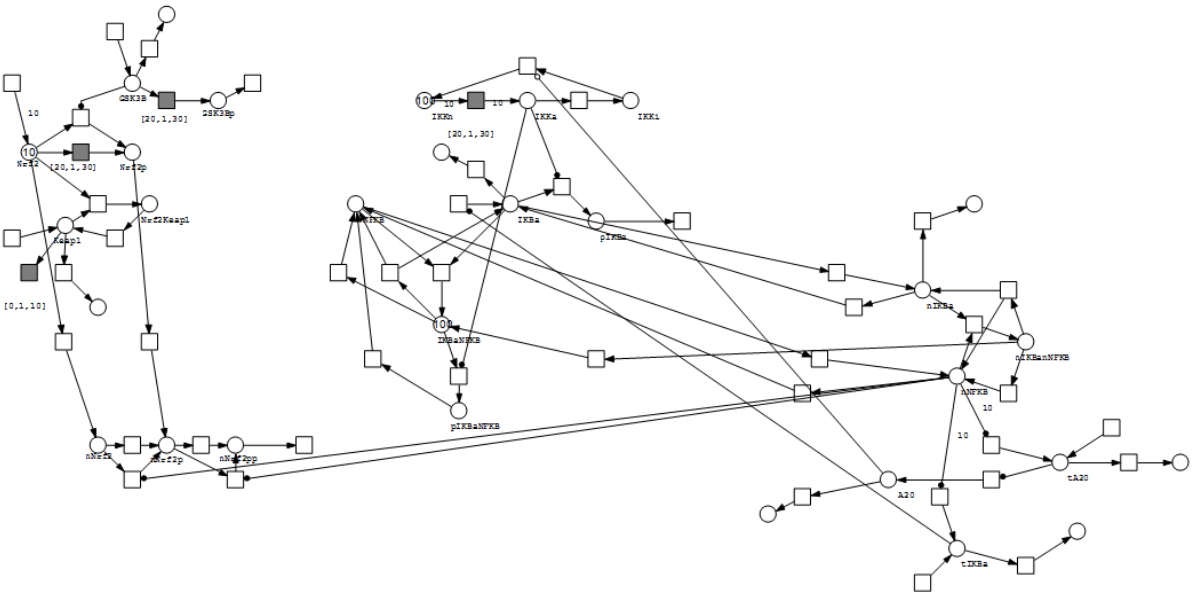

Figure 1: Bipartite graphic notation for both NFkB and Nrf2, this graphical notation is representative for variation number 2.

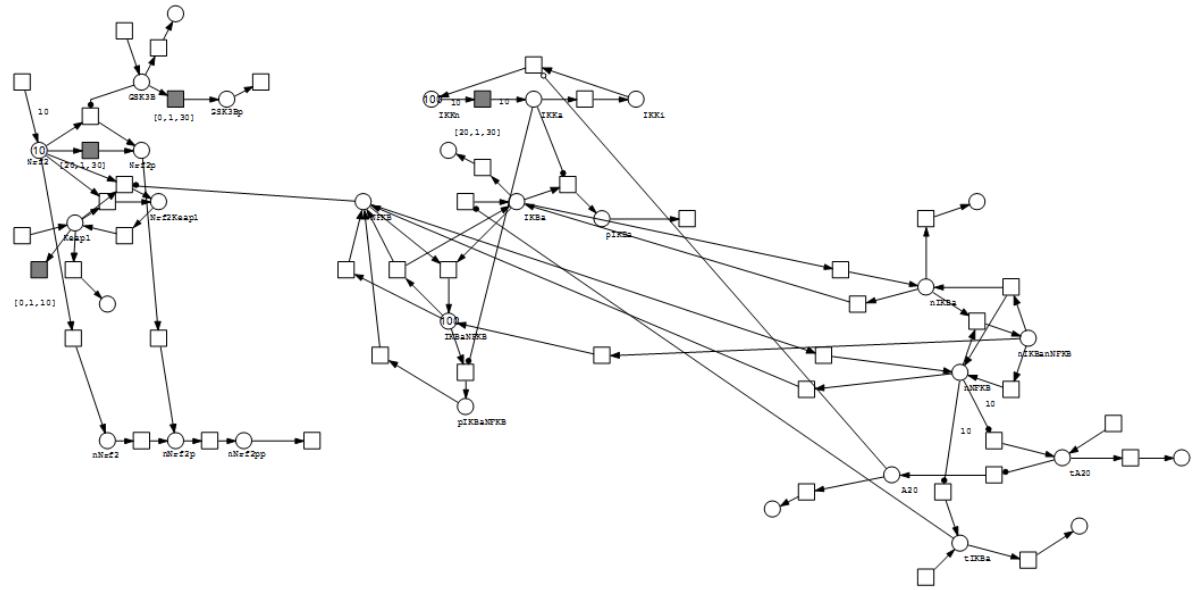

Figure 1: Bipartite graphic notation for both NFkB and Nrf2, this graphical notation is representative for variation number 3.

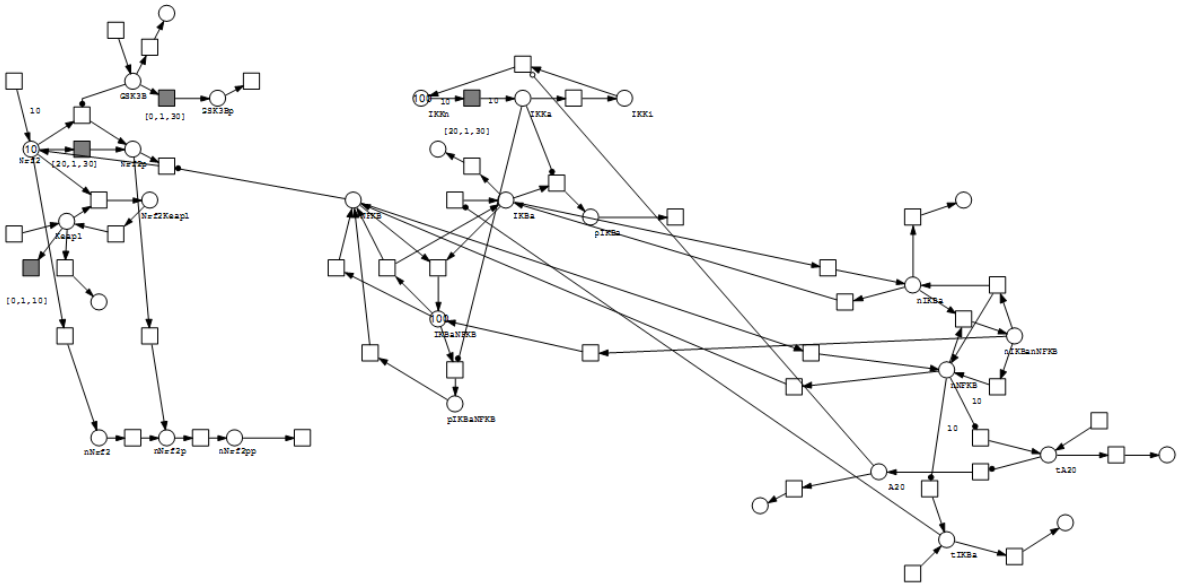

Figure 1: Bipartite graphic notation for both NFkB and Nrf2, this graphical notation is representative for variation number 4.

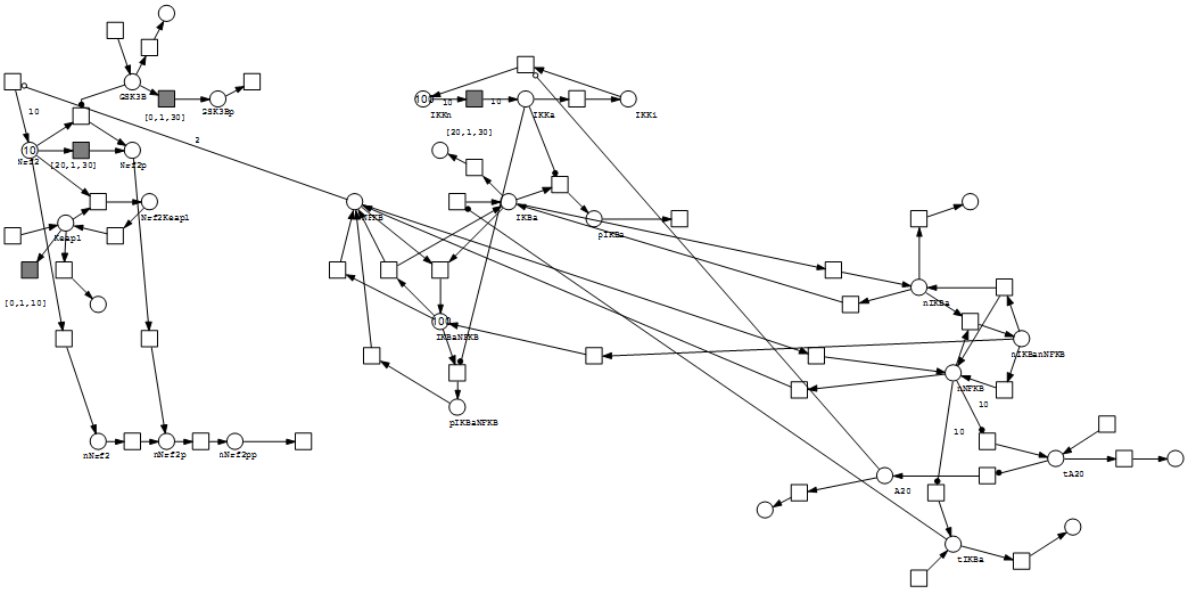

Figure 1: Bipartite graphic notation for both NFkB and Nrf2, this graphical notation is representative for variation number 5.